

# Few-Layer Graphene Kills Selectively Tumor Cells from Myelomonocytic Leukemia Patients

Julie Russier, Verónica León, Marco Orecchioni, Eri Hirata, Patrizia Viridis, Claudio Fozza, Francesco Sgarrella, Gianaurelio Cuniberti, Maurizio Prato, Ester Vázquez,\* Alberto Bianco,\* and Lucia G. Delogu\*

**Abstract:** In the cure of cancer, a major cause of today's mortality, chemotherapy is the most common treatment, though serious frequent challenges are encountered by current anticancer drugs. We discovered that few-layer graphene (FLG) dispersions have a specific killer action on monocytes, showing neither toxic nor activation effects on other immune cells. We confirmed the therapeutic application of graphene on an aggressive type of cancer that is myelomonocytic leukemia, where the monocytes are in their malignant form. We demonstrated that graphene has the unique ability to target and boost specifically the necrosis of monocytic cancer cells. Moreover, the comparison between FLG and a common chemotherapeutic drug, etoposide, confirmed the higher specificity and toxicity of FLG. Since current chemotherapy treatments of leukemia still cause serious problems, these findings open the way to new and safer therapeutic approaches.

The scientific and medical battle against cancer remains one of the biggest challenges of our times. Cancer is still one of the major causes of mortality.<sup>[1]</sup> The blood-related cancers, such as leukemia in its multiple variants, are among those ones with the highest incidence of mortality.<sup>[2]</sup> Acute myeloid leukemia (AML) and chronic myelomonocytic leukemia (CMML) represent two different subtypes of the so called myeloid neoplasms.<sup>[3]</sup> This type of cancer is usually dominated by the rapid growth of abnormal immature white blood cell precursors that accumulate in bone marrow and peripheral blood interfering with the normal hematopoietic function.<sup>[4,5]</sup>


Both AML and CMML are characterized by circulating monocytic neoplastic cells. The conventional treatment of these disorders is usually based on different chemotherapeutic regimens, which are often characterized by disappointing remission rates especially in elderly patients. Traditional therapies to counteract cancer in general, and also myelomonocytic leukemia, are limited by multiple problems, including nonspecific systemic distribution of antitumor agents, inadequate drug concentrations reaching the tumor site, intolerable cytotoxicity, limited ability to monitor the therapeutic responses, and development of multiple drug resistance.<sup>[6]</sup>

In this scenario, nanotechnology could be the hoped medical revolution allowing to treat cancer effectively, reducing undesired side effects.<sup>[7]</sup> The development of new nanomaterials endowed of unique properties could represent a strong enhancement in the cure of cancer. Graphene is one of the nanomaterials that has raised tremendous interest in the scientific community and the society.<sup>[8]</sup> Graphene is being explored for many potential applications due to its exceptional physicochemical characteristics.<sup>[9]</sup> Very recently, different types of graphene have been investigated in a growing number of medical applications, including drug delivery, diagnosis, tissue engineering and gene transfection.<sup>[10]</sup>

In this work, we studied FLG dispersions<sup>[11]</sup> and discovered a highly specific toxicity on primary human monocytes. Based on this interesting result, we evaluated the killing activity of graphene in monocytic neoplastic cells from a cohort of AML and CMML patients.

[\*] J. Russier, E. Hirata, A. Bianco  
University of Strasbourg, CNRS  
Immunopathology and therapeutic chemistry, UPR 3572  
67000 Strasbourg (France)  
E-mail: a.bianco@ibmc-cnrs.unistra.fr  
V. León, E. Vázquez  
Departamento de Química Orgánica  
Facultad de Ciencias y Tecnologías Químicas-IRICA  
Universidad de Castilla-La Mancha  
13071 Ciudad Real (Spain)  
E-mail: Ester.Vazquez@uclm.es  
M. Orecchioni, F. Sgarrella, L. G. Delogu  
Department of Chemistry and Pharmacy  
University of Sassari  
07100 Sassari (Italy)  
E-mail: lgdelogu@uniss.it  
E. Hirata  
Department of Oral Functional Science  
Graduate School of Dental Medicine  
Hokkaido University  
060-8586, Sapporo (Japan)

P. Viridis, C. Fozza  
Department of Clinical and Experimental Medicine  
University of Sassari  
07100 Sassari (Italy)  
G. Cuniberti, L. G. Delogu  
Max Bergmann Center of Biomaterials and  
Institute for Materials Science, Dresden University of Technology  
01069 Dresden (Germany)  
M. Prato  
Dipartimento di Scienze Chimiche e Farmaceutiche  
Università di Trieste, 34127 Trieste (Italy)  
and  
CIC BiomaGUNE, Parque Tecnológico de San Sebastián  
Paseo Miramón, 182, 20009 San Sebastián (Guipúzcoa) (Spain)  
and  
Basque Foundation for Science  
Ikerbasque, 48013 Bilbao (Spain)

 Supporting information for this article can be found under:  
<http://dx.doi.org/10.1002/anie.201700078>.

The majority of the biomedical studies using graphene-based nanomaterials have focused on graphene oxide, while there are only a limited number of biological studies on graphene.<sup>[12]</sup> The reason for this is the difficulty to disperse graphene directly in water or in culture media. In this context, we have prepared few-layer graphene by exfoliation of graphite through interaction with melamine using a ball-milling process, under solvent-free conditions.<sup>[11]</sup> This methodology allows to produce three–four layer graphene dispersions in water ( $0.1 \text{ mg mL}^{-1}$ ). Moreover, water can be easily replaced by filtration or lyophilization with cell culture medium to form stable graphene dispersions.<sup>[13]</sup> Figure 1 shows the relevant characterization data of the FLG material.

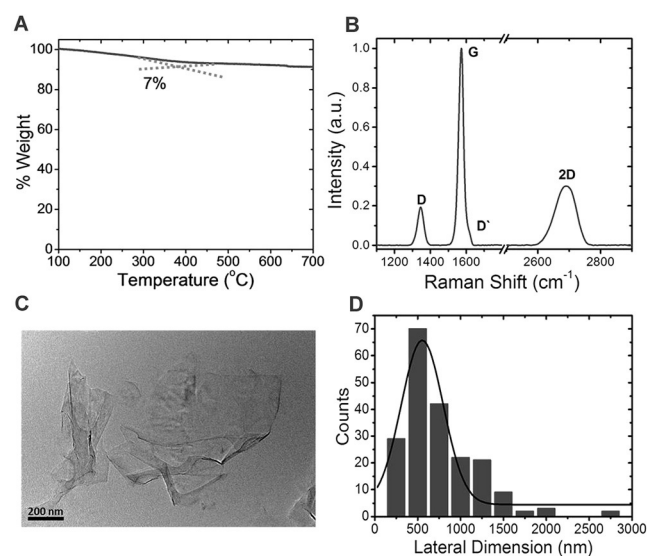


**Figure 1.** Characterization of FLG. A) Thermogravimetric analysis. B) Normalized Raman spectrum. C) TEM image of FLG in cell culture medium and D) lateral dimension distribution.

Thermogravimetric analysis (TGA) was used to quantify the presence of functional groups in FLG (Figure 1 A). The low weight loss observed in FLG (7 %) confirms the low quantity of oxygen groups generated during the exfoliation process, which was also corroborated by elemental analysis (see the Experimental Section in the Supporting Information). Further proof of the non-oxidative milling process was confirmed by Raman spectroscopy (Figure 1B and the Supporting Information). Graphene exhibits G and 2D modes around  $1573$  and  $2700 \text{ cm}^{-1}$ , respectively. The D/G band intensity ratio, used to quantify the defects, was calculated at different topographies, giving a significantly low value (0.2). A representative TEM image of FLG dispersions in cell culture medium is shown in Figure 1C, evidencing the typical wrinkled aspect of the graphene flakes. Statistical analysis of TEM images afforded a major population with a lateral size about  $500\text{--}750 \text{ nm}$ , with a small fraction above  $2000 \text{ nm}$  (Figure 1D). Additional XPS data are shown in Figure S1 in the Supporting Information.

FLG stable in cell culture media resulted immediately an interesting material to study its impact on primary human

immune cells. The use of these cells is at the forefront in the study of the effects of new materials in a biomedical or toxicological context.<sup>[7c,14]</sup> For this purpose, we analyzed the impact of FLG on peripheral blood mononuclear cell (PBMC) populations looking at T, B, NK, dendritic cells, and monocytes. The cells were treated with different doses of FLG from  $0.5 \mu\text{g mL}^{-1}$  to  $75 \mu\text{g mL}^{-1}$  for 24 h (Figure S2), which we consider the optimal time for graphene cellular internalization, and were analyzed by flow cytometry.<sup>[14b,15]</sup> Very interestingly, we found a specific cytotoxic activity of FLG on monocytes ( $\text{CD14}^+$  cells), while the percentage of events reported for T, B, NK, and dendritic cells remained unchanged. This effect is appreciable also in the dot plots, where the positive events for  $\text{CD14}^+$  completely disappeared (Figure 2), and it was not due to the presence of residual melamine (Figure S3). The other immune cell populations remained unaffected in terms of cell viability (Figure S4). The

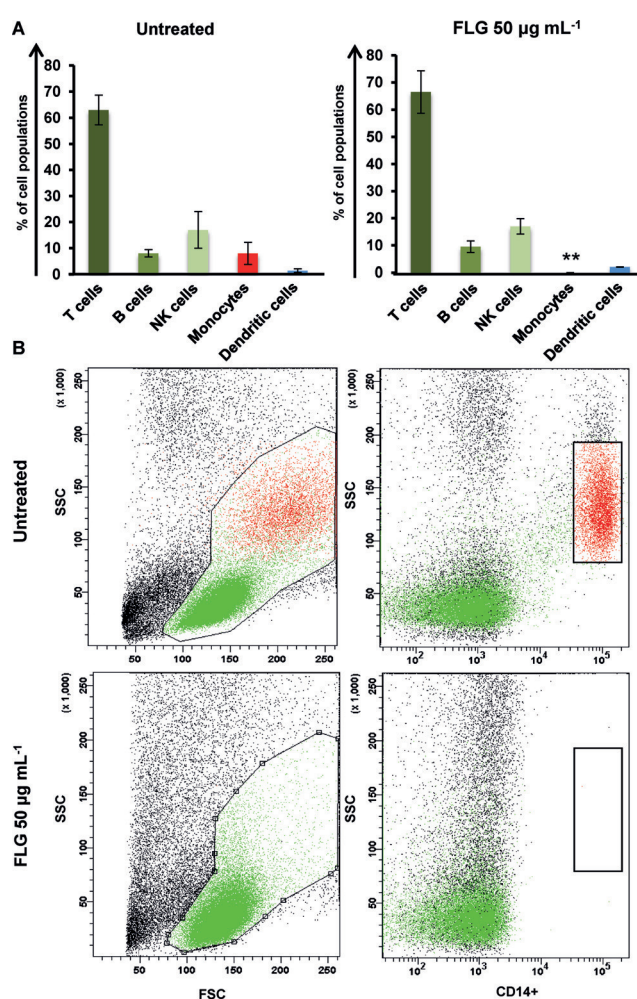


**Figure 2.** Impact of FLG on different immune cell populations. A) Relative percentage of the different immune cells either incubated for 24 h with  $50 \mu\text{g mL}^{-1}$  FLG or left untreated. Statistical significance compared to untreated cells (Student's T-test) is indicated by \*\* =  $p < 0.01$ . B) Relative morphological dot plots out of at least three experiments of total PBMCs treated with FLG or left untreated. The gate on monocytes was done looking at the  $\text{CD14}^+$  positive events (red dots). The other immune populations are left in green.

highly specific effect of FLG was also confirmed by evidencing its non-cytotoxic impact on other types of cells (Figure S5).

As we could not record any direct activation of monocytes (i.e. no significant increase of CD86 expression, Figure S6), we decided to investigate whether an indirect activation of monocytes via the activation of T cells was occurring. Indeed, FLG-mediated activation of T cells could induce a strong stimulation of monocytes triggering their death.<sup>[16]</sup> We analyzed the expression of specific lymphocyte activation markers, namely CD25 and CD69. Their expression in FLG-exposed samples was comparable to the untreated negative controls (Figure S7). These data exclude any T cell activation mediated by FLG. The absence of activation of the T cells suggested a direct action of FLG on monocytes. The hypothesis of a selective activity of the FLG towards monocytes is consistent with the transmission electron microscopy (TEM) analysis on total PBMCs (Figure S8). The fact that only monocytes are able to internalize FLG could explain our results on cellular activation and cytokine production. Other reports showed an effect of graphene, and in particular of GO, on macrophages or DCs.<sup>[17]</sup> However, none of them reported such strong specific killing on monocyte compared to other immune cell populations. In fact we evidenced that treatments of PBMCs with a commercial graphene oxide do not affect the monocyte population (Figure S9).<sup>[18]</sup>

We then investigated the cell death on monocytes isolated from PBMCs. Monocytes were treated with FLG at  $50 \mu\text{g mL}^{-1}$  and at different time points (1, 4, 12, and 24 h) to analyze the induced specific death processes (Figure S10A). The morphological dot plots (Figure S10B) show the progressive reduction of monocytes (CD14<sup>+</sup> cells). Even at early time points (1 and 4 h) of incubation a significant induction of dead cells was observed (Figure S10C). The necrotic cells increased also significantly from 6.2% in the control sample to 29% after 1 h and 36.5% after 4 h (Figure S10A). Mortality of monocytes reached 71.3% after 24 h of incubation with FLG ( $P\text{-value} < 0.01$ ). We also observed the absence of a significant number of apoptotic cells in all FLG treated samples (Figure S10A) suggesting that graphene directly triggers necrosis on monocytes.

To investigate the mechanisms of FLG mediated cell death we first performed a whole-genome expression, looking at more than 41,000 transcripts on isolated monocytes from healthy patients. Venn diagram in Figure S11A shows the number of genes that passed the cutoff at the different time points. As expected the number of genes modulated by FLG increased from 773 after 30 minutes to 836 and 966 after 90 and 270 minutes, respectively. The genes up-regulated by FLG were mainly chemokines (i.e. CCL1, CCL2, CCL8, CCL19, CLCL4L2, CXCL1 and CXCL3) and cytokines (i.e. IL-23a, IL-6, IL-1a, TNF, CSF2 and CSF3) (Table S1). They all account for the activation process played by FLG on monocytes that increased proportionally with incubation time. To understand the biological function of FLG we then performed a pathway analysis. Figure S11B displays the 10 most significantly modulated pathways corresponding to IL-10, IL-6 and TREM1 signaling. All these pathways confirmed

again the activating action of FLG on monocytes. IL-10 signaling pathway is in general induced by the activation of toll-like receptors (TLR) 2 and 4 with the regulation of the inflammation through the inhibition of pro-inflammatory cytokines TNF $\alpha$  and IL-6.<sup>[19]</sup> It was previously evidenced how the internalization of graphene could be mediated by TLR2 and TLR4.<sup>[18a]</sup> The toxicity of our FLG is likely induced by the activation of both TLR signaling via TNF $\alpha$  production.<sup>[19,20]</sup> To investigate whether TLR2/TLR4 receptors were involved in the selective cytotoxic effect of FLG on monocytes, we analyzed ex vivo the monocytes treated with and without TLR2/TLR4 blocking antibodies. The experiments revealed that TLR4 seems not or only partially involved in the mechanism inducing selective cell death of monocyte by FLG (Figure S12A). Instead, the inhibition of TLR2 blocked the expression of CD25 in treated monocytes (Figure S12B). Moreover, the inhibition of TLR2 was able to restore the number of monocytes compared to the controls. Together with the gene expression analysis, these results suggest that the FLG toxicity on monocytes is mediated by the interaction of FLG with TLR2 and the subsequent expression of TNF $\alpha$  and TNFR family (see also the Supporting Information).<sup>[21]</sup>

The high selective capacity of our FLG to kill human monocytes is promising for the treatment of myelomonocytic leukemia, which presents high percentages of circulating monocytic neoplastic cells. Therefore, we analyzed the effect of FLG as a new chemotherapeutic tool in myeloid malignancies. In particular, we evaluated the monocytoid CD14<sup>+</sup> cell viability in PBMCs obtained from a cohort of seven patients (6 male and 1 female) with a median age of 70, newly diagnosed with AML or CMML, before starting the therapeutic treatment (Figure 3). The presence of FLG accumulated into the monoblasts (Figure S13A) was observed into the peripheral blood smear of AML (Figure S13B) and CMML (Figure S13C) patients. PBMCs of the patients were then treated with increasing doses of FLG to assess the capacity of graphene to specifically kill the neoplastic monocytes. In the untreated samples of all patients (Figure 3), two peaks of cells are well visible: the first on the left comprises all cells negative to the CD14 marker corresponding to non-neoplastic cells (i.e. T cells, B cells, NK and dendritic cells), while the peak on the right identifies CD14<sup>+</sup> monocytoid cancer cells. After the treatment with FLG, the cancer cell population was strongly reduced in all AML and CMML patients in an FLG concentration dependent manner with no effect on the other immune cells (Figure 3). We would like to point out that in the 6 patients, the number of cancer cells was strongly reduced even at low concentrations ( $0.5$  and  $5 \mu\text{g mL}^{-1}$ ) with two fold, and three fold average decrease, respectively. Regarding the ablation obtained at  $25$  and  $50 \mu\text{g mL}^{-1}$ , the percentage of cells was extremely reduced from an average of 24% to an average of 2.2% and 1.6%, respectively (Figure 3 and Figure S14). In particular, patient 4 was characterized by a critical condition with an extremely high number of monocytoid cancer cells comparable to all other immune cells. The treatment with FLG even at the lower concentrations has shown 40% and 83% reduction of the neoplastic cell number, reaching the total ablation at  $25 \mu\text{g mL}^{-1}$  (Figure 3, Pt.4). The analysis of



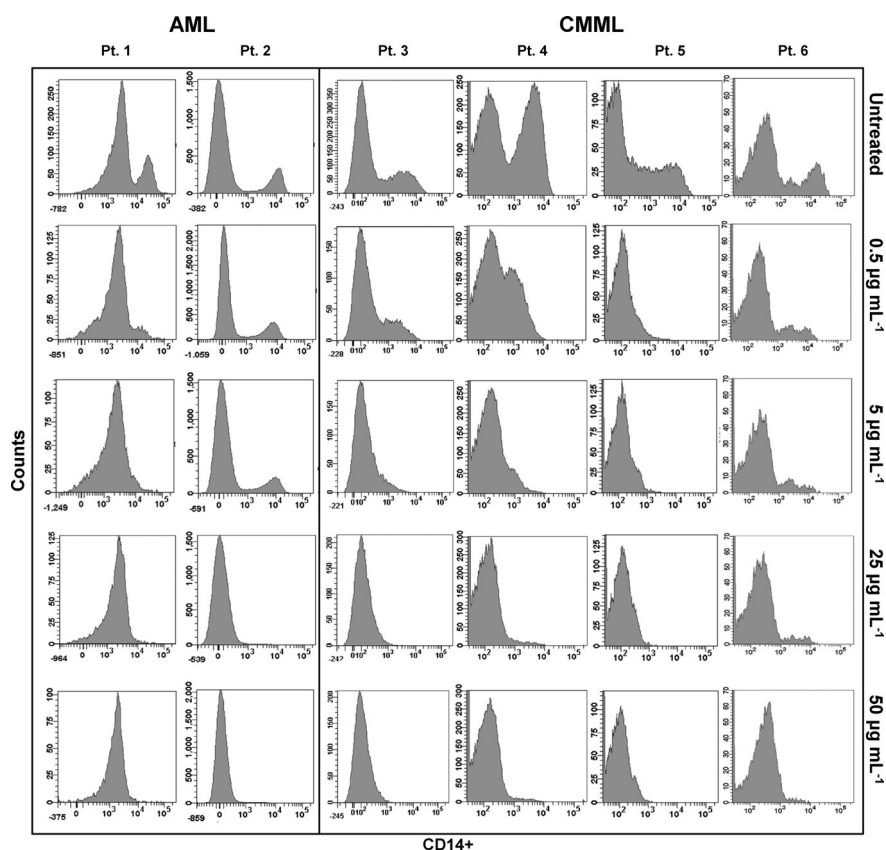


**Figure 3.** FLG impact on ex vivo PBMCs from AML and CMML patients. Monocytoid cells were highlighted by CD14 positivity (right peaks), the other populations were negative (left peaks).

the cytokine secretion in CMML patients after the treatment with FLG did not evidence any induction of inflammatory processes in other immune cells. Thus, only monocyte-associated cytokines were found overexpressed under FLG treatment (Figure S15).

Furthermore, we compared the specific effect of FLG with etoposide, a common chemotherapeutic agent clinically used in the treatment of both AML and CMML. Etoposide was specifically selected because of its ability to selectively induce monocytopenia, the deficiency of monocytes mandatory to prevent tumor expansion.<sup>[22]</sup> We tested concentration of etoposide between 50 and 200  $\mu\text{M}$ , normally used to treat AML and CMML.<sup>[23]</sup> The comparison of the effect of FLG at 50  $\mu\text{g mL}^{-1}$  with the different etoposide doses in PBMCs isolated from AML patients underlines the safety use of FLG with no toxic effect on the other immune cell populations (Figure 4A). As expected, etoposide induced a significant T, B and NK cell toxicity at all concentrations (Figure 4A). In B cells, we found a 49.6% of dead cells at the lowest concentration and a 68.3% at the highest. We further confirmed the strong specific effect of FLG on neoplastic CD14<sup>+</sup> cells compared to etoposide (Figure 4B). These findings open the way to a possible application of FLG as a specifically targeted tool against neoplastic cells in AML and CMML. This new therapeutic strategy based on graphene might be extremely advantageous over the traditional treatments using conventional chemotherapeutic agents such as etoposide, cytarabine,

anthracyclines or hydroxyurea,<sup>[4,5]</sup> that are non specific and impair all immune cell subpopulations, causing possible infections and death. Moreover, some of these chemotherapies act by activating the apoptosis pathway in tumor cells. Paradoxically, the fact that anti-cancer agents are effective primarily because they activate apoptosis raises the concern that tumors intrinsically resistant to chemotherapy are unable to activate the apoptotic machinery and may be resistant to any chemotherapeutic drug.<sup>[24]</sup> The necrosis-mediated action of FLG could avoid the resistance of tumor cells.

Finally, given the complexity of the toxicology and pharmacokinetic issues with graphene-based materials, we characterized the systemic body reaction to FLG in vivo. All injected mice behaved normally and did not show signs of adverse reactions (see Figure S16).

In summary, in this work, we found a specific toxicity of FLG on primary human monocytes. In particular, we demonstrated a unique ability of graphene to target and successfully boost the necrosis of monocytoid cancer cells for acute myeloid leukemia and chronic myelomonocytic leukemia patients.

Moreover, the comparison between FLG and a common chemotherapeutic drug confirmed the specificity and higher toxicity of FLG on cancer cells, evidencing the absence of toxicity on other immune cell populations. Considering the FLG specific ability to target and kill cancer cells of an aggressive form of malignancy, extremely promising potentials as a new cancer tool can be envisaged for graphene.

### Acknowledgements

This work was partly supported by the Italian Association against Leukemia (AIL), by the Centre National de la Recherche Scientifique, by the Ministerio de Economía y competitividad CTU2014-53600-R and by the Japan Society for the Promotion of Science through a Research Fellowship for Young Scientists (grant number 24006076). The authors gratefully acknowledge financial support from EU FP7-ICT-2013-FET-F GRAPHENE Flagship project (number 604391) and from MIUR JTC Graphene 2015 (G-IMMUNOMICS project). E.V. thanks Emilio Pérez and Viviana Jehová González (IMDEA Nanociencia, Madrid) for the Raman measurements.

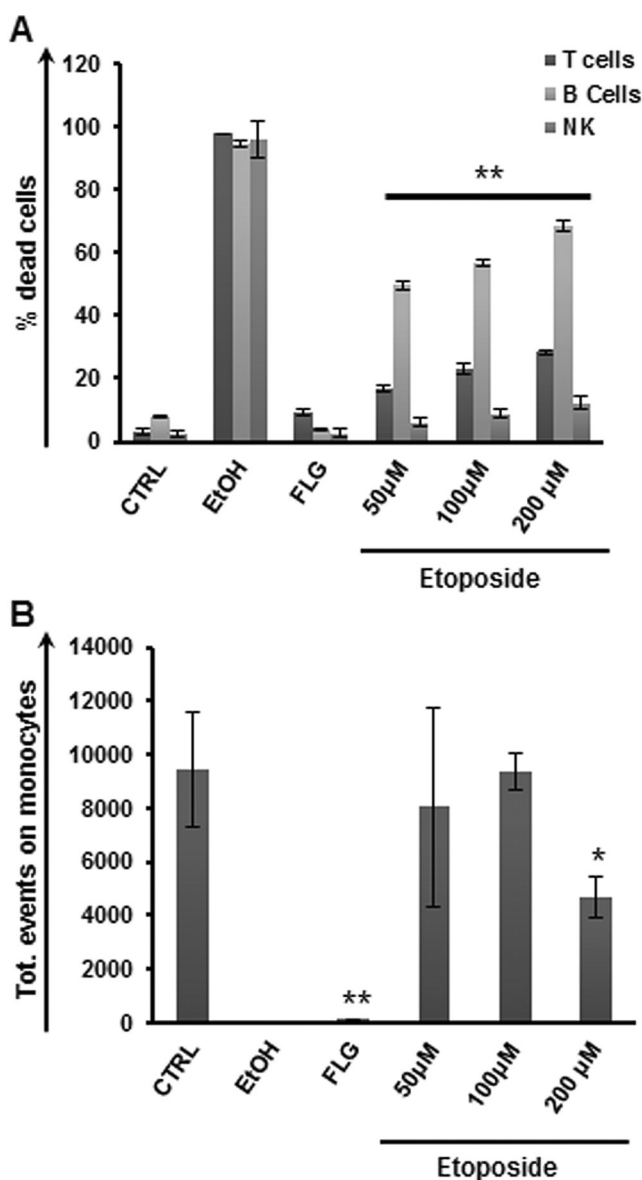


**Figure 4.** Comparison between etoposide and FLG on PBMCs from AML patients. PBMCs were incubated with 50  $\mu$ g mL<sup>-1</sup> FLG and etoposide at different concentrations. After 24 h the cells were harvested and stained with a viability marker dye (7AAD). A) Viability screening of different immune cell populations (i.e. T, B, and NK cells). B) Count of monocytoic cells (CD14<sup>+</sup>) treated with FLG (50  $\mu$ g mL<sup>-1</sup>) and etoposide or left untreated. Statistical significance compared to untreated cells (student's t test) is indicated by \* =  $p < 0.05$  and \*\* =  $p < 0.01$ .

## Conflict of interest

The authors declare no conflict of interest.

**Keywords:** cancer therapy · graphene · immune system · myelomonocytic leukemia · nanomaterials

- [1] M. López-Gómez, E. Malmierca, M. de Górgolas, E. Casado, *Crit. Rev. Oncol. Hematol.* **2013**, *88*, 117–122.
- [2] N. Holler, R. Zaru, O. Micheau, M. Thome, A. Attinger, S. Valitutti, J. L. Bodmer, P. Schneider, B. Seed, J. Tschoopp, *Nat. Immunol.* **2000**, *1*, 489–495.
- [3] J. W. Vardiman, J. Thiele, D. A. Arber, R. D. Brunning, M. J. Borowitz, A. Porwit, N. L. Harris, M. M. Le Beau, E. Hellstrom-Lindberg, A. Tefferi, C. D. Bloomfield, *Blood* **2009**, *114*, 937–951.
- [4] H. Dohner, D. J. Weisdorf, C. D. Bloomfield, *N. Engl. J. Med.* **2015**, *373*, 1136–1152.
- [5] C. B. Benton, A. Nazha, N. Pemmaraju, G. Garcia-Manero, *Crit. Rev. Oncol. Hematol.* **2015**, *95*, 222–242.
- [6] a) R. Misra, S. Acharya, S. K. Sahoo, *Drug Discovery Today* **2010**, *15*, 842–850; b) G. Szakács, J. K. Paterson, J. A. Ludwig, C. Booth-Genthe, M. M. Gottesman, *Nat. Rev. Drug Discovery* **2006**, *5*, 219–234.
- [7] a) M. S. Goldberg, *Cell* **2015**, *161*, 201–204; b) M. Orecchioni, R. Cabizza, A. Bianco, L. G. Delogu, *Theranostics* **2015**, *5*, 710–723; c) M. Pescatori, D. Bedognetti, E. Venturelli, C. Menard-Moyon, C. Bernardini, E. Muresu, A. Piana, G. Maida, R. Manetti, F. Sgarrella, A. Bianco, L. G. Delogu, *Biomaterials* **2013**, *34*, 4395–4403.
- [8] a) G. Sechi, D. Bedognetti, F. Sgarrella, L. Van Eperen, F. M. Marincola, A. Bianco, L. G. Delogu, *Nanomedicine* **2014**, *9*, 1475–1486.
- [9] A. K. Geim, K. S. Novoselov, *Nat. Mater.* **2007**, *6*, 183–191.
- [10] a) L. Zhang, J. Xia, Q. Zhao, L. Liu, Z. Zhang, *Small* **2010**, *6*, 537–544; b) L. Feng, S. Zhang, Z. Liu, *Nanoscale* **2011**, *3*, 1252–1257; c) S. Dinescu, M. Ionita, A. M. Pandele, B. Galateanu, H. Iovu, A. Ardelean, M. Costache, A. Hermenean, *Bio-Med. Mater. Eng.* **2014**, *24*, 2249–2256; d) S. Jaworski, E. Sawosz, M. Grodzik, A. Winnicka, M. Prasek, M. Wierzbicki, A. Chwalibog, *Int. J. Nanomed.* **2013**, *8*, 413–420.
- [11] V. León, M. Quintana, M. A. Herrero, J. L. Fierro, A. de la Hoz, M. Prato, E. Vázquez, *Chem. Commun.* **2011**, *47*, 10936–10938.
- [12] M. Orecchioni, C. Menard-Moyon, L. G. Delogu, A. Bianco, *Adv. Drug Deliv. Rev.* **2016**, *105*, 163–175.
- [13] V. León, J. M. González-Domínguez, J. L. Fierro, M. Prato, E. Vázquez, *Nanoscale* **2016**, *8*, 14548–14555.
- [14] a) J. Russier, E. Treossi, A. Scarsi, F. Perrozzi, H. Dumortier, L. Ottaviano, M. Meneghetti, V. Palermo, A. Bianco, *Nanoscale* **2013**, *5*, 11234–11247; b) M. Orecchioni, D. A. Jasim, M. Pescatori, R. Manetti, C. Fozza, F. Sgarrella, D. Bedognetti, A. Bianco, K. Kostarelos, L. G. Delogu, *Adv. Healthcare Mater.* **2016**, *5*, 276–287.
- [15] Y. Li, H. Yuan, A. von dem Bussche, M. Creighton, R. H. Hurt, A. B. Kane, H. Gao, *Proc. Natl. Acad. Sci. USA* **2013**, *110*, 12295–12300.
- [16] C. A. Roberts, A. K. Dickinson, L. S. Taams, *Front. Immunol.* **2015**, *6*, 571.
- [17] Y. Li, Y. Liu, Y. J. Fu, T. T. Wei, L. Le Guyader, G. Gao, R. S. Liu, Y. Z. Chang, C. Y. Chen, *Biomaterials* **2012**, *33*, 402–411.
- [18] a) G. Ou, S. Liu, S. Zhang, L. Wang, X. Wang, B. Sun, N. Yin, X. Gao, T. Xia, J. J. Chen, G. B. Jiang, *ACS Nano* **2013**, *7*, 5732–5745; b) A. Sasidharan, L. S. Panchakarla, A. R. Sadanandan, A. Ashokan, P. Chandran, C. M. Girish, D. Menon, S. V. Nair, C. N. Rao, M. Koyakutty, *Small* **2012**, *8*, 1251–1263; c) A. V. Tkach, N. Yanamala, S. Stanley, M. R. Shurin, G. V. Shurin, E. R. Kisin, A. R. Murray, S. Pareso, T. Khaliullin, G. P. Kotchey, V. Castranova, S. Mathur, B. Fadeel, A. Star, V. E. Kagan, A. A. Shvedova, *Small* **2013**, *9*, 1686–1690.
- [19] Y. Yanagawa, K. Onoé, *J. Immunol.* **2007**, *178*, 6173–6180.
- [20] F. Marques-Fernandez, L. Planells-Ferrer, R. Gozzelino, K. M. Galenkamp, S. Reix, N. Llecha-Cano, J. Lopez-Soriano, V. J.

- Yuste, R. S. Moubarak, J. X. Comella, *Cell Death Dis.* **2013**, *4*, e493.
- [21] A. O. Aliprantis, R.-B. Yang, D. S. Weiss, P. Godowski, A. Zychlinsky, *EMBO J.* **2000**, *19*, 3325–3336.
- [22] J. W. Van't Wout, I. Linde, P. C. Leijh, R. van Furth, *Inflammation* **1989**, *13*, 1–14.
- [23] a) A. Montecucco, F. Zanetta, G. Biamonti, *EXCLI J.* **2015**, *14*, 95–108; b) M. A. Papiez, W. Krzysciak, K. Szade, K. Bukowska-Strakova, M. Kozakowska, K. Hajduk, B. Bystrowska, J. Dulak, A. Jozkowicz, *Drug. Des. Dev. Ther.* **2016**, *10*, 557–570.
- [24] Y. A. Hannun, *Blood* **1997**, *89*, 1845–1853.
- Manuscript received: January 4, 2017  
Final Article published: February 3, 2017
-